Synthesis, Crystal Structure, and Properties of a Polyimidazole Diiron(III) Complex. A New Model of the Active Site of Purple Acid Phosphatase

Hanlin Nie,[†] Sheila M. J. Aubin,[‡] Mark S. Mashuta,[†] Chi-Cheng Wu,[‡] John F. Richardson,[†] David N. Hendrickson,*[,‡] and Robert M. Buchanan*[,†]

Departments of Chemistry, University of Louisville, Louisville, Kentucky 40292, and University of California at San Diego, La Jolla, California 92093

Received November 1, 1994[⊗]

The synthesis and characterization of a new dinuclear iron(III) complex formed during the reaction of the septadentate ligand 2,6-bis[((2-hyroxybenzyl)((1-methylimidazol-2-yl)methyl)amino)methyl]-4-methylphenol (H_3-BIOMP) are reported. The crystal structure of the complex has been solved. The μ-phenolate bis(μ-acetate) diiron(III) complex $[Fe_2(BIOMP)(\mu\text{-}O_2CCH_3)_2](ClO_4)\cdot H_2O$ (**5**) crystallizes in the space group $P2_1/n$ with cell dimensions $a = 14.983(14)$ Å, $b = 12.341(13)$ Å, $c = 21.391(16)$ Å, $\beta = 90.79(7)°$, $V = 3955(6)$ Å^3, and $Z = 4$ and was solved for 3493 reflections [$I > 3\sigma(I)$], giving $R = 6.7\%$ and $R_w = 8.3\%$. The compound consists of two iron(III) ions bridged by a phenolate oxygen atom and coordinated each to phenol, amine, and imidazole pendants of the septadentate ligand as well as bridging acetate ions. The cation has approximately C_2 symmetry. The iron(III) ions are weakly coupled antiferromagnetically ($J = -6.34$ cm^{-1}) and undergo quasireversible one-electron redox processes. The $Fe^{II}_2/Fe^{II}Fe^{III}$ and $Fe^{II}Fe^{III}/Fe^{III}_2$ couples are at −0.785 and −0.225 V vs Ag/AgCl, respectively. Compound **5** also displays an intense phenolate-to-iron(III) charge transfer transition at 586 nm ($\epsilon = 7400$ M^{-1} cm^{-1}/Fe$_2$). The ^{57}Fe Mössbauer spectra of **5** were recorded at 295 and 125 K, and both display a single quadrupolar split doublet. The quadrupole splitting (ΔE_Q) is equal to 1.083(23) mm/s at 295 K and 1.055 (9) mm/s at 125 K. The isomer shift (δ) parameters at 295 and 125 K are 0.406(13) and 0.508(5) mm/s, respectively.

Introduction

Several non-heme iron proteins are known to contain oxo-bridged dinuclear active sites which are capable of stabilizing Fe^{II}_2, $Fe^{II}Fe^{III}$, and Fe^{III}_2 oxidation levels. The structures of these biomolecules and their physical properties have been the subject of intense investigation.[1] Crystal structures of the oxidized forms of hemerythrin (Hr),[2] ribonucleotide reductase (RNR R2),[3] and methane monooxygenase (MMO)[4] are known. Hemerythrin and methane monooxygenase have bis(μ-carboxylato)(μ-oxo)- and bis(μ-carboxylato)(μ-hydroxo)-bridged structures, respectively, whereas ribonucleotide reductase has a (μ-carboxylato)-(μ-oxo)-bridged core structure. The active site structures of purple acid phosphatase (PAP) and the related glycoproteins from bovine spleen (BSPAP) and porcine uteri (uteroferrin (Uf)), on the other hand, are not known but are thought to have similar core structures containing bridging hydroxo ligands.

Non-heme oxo−iron proteins participate in a number of loosely related reactions ranging from O_2 transport (Hr) to alkane functionalization reactions (MMO). PAPs catalyze the hydrolysis of phosphate esters and readily stabilize two oxidation levels of the iron centers. Interestingly, the phosphatase enzymes are inactivated by dioxygen in the presence of phosphate ion. The catalytically active mixed-valence $Fe^{II}Fe^{III}$ form of the protein is pink ($\lambda_{max} = 510$ nm, $\epsilon = 4000$ M^{-1} cm^{-1}) and displays a rhombic EPR signal ($g_{av} = 1.74$)[5] while the catalytically inactive and EPR-silent Fe^{III}_2 form ($\lambda_{max} = 560$ nm, $\epsilon = 4000$ M^{-1} cm^{-1}) is purple.[6,7] The fact that visible chromophores associated with both oxidation levels of the protein originate from a tyrosine-to-iron(III) charge-transfer transition and have similar extinction coefficients suggests that the tyrosine residue is bonded to only one iron center.[6,8] Recent EXAFS[9] and resonance Raman studies on Uf[8] and BSPAP[6] established the absence of a bridging Fe−O−Fe unit in both the reduced and oxidized forms of the proteins and suggested that the iron centers are bonded to 3.5 N/O donors at about 2.14 Å, which are likely associated with imidazole (histidine) and carboxylate (aspartate or glutamate) amino acid residues as well as possibly a water molecule. NMR studies have provided further evidence for an additional bridging group (carboxylate) as well as terminal imidazole and carboxylate ligands.[10] The apparent simplicity of the activities of these

* Authors to whom correspondence should be addressed.
[†] University of Louisville.
[‡] University of California at San Diego.
[⊗] Abstract published in *Advance ACS Abstracts,* April 1, 1995.

(1) (a) Klotz, I. M.; Kurtz, D. M., Jr. *Acc. Chem. Res.* **1984**, *17*, 16−22. (b) Wilkins, P. C.; Wilkins, R. G. *Coord. Chem. Rev.* **1987**, *79*, 195−214. (c) Fox, B. G.; Sererus, K. K.; Münck, E.; Lipscomb, J. D. *Biol. Chem.* **1988**, *22*, 10553−10556. (d) Lippard, S. J. *Angew. Chem., Int. Ed. Engl.* **1988**, *27*, 344− 361. (e) Que, L., Jr. *ACS Symp. Ser.* **1988**, *372*, 152−178. (f) Vincent, J. B.; Olivier-Lilley, G. L.; Averill, B. A. *Chem. Rev.* **1990**, *90*, 1447−1467. (g) Kurtz, D. M., Jr. *Chem. Rev.* **1990**, *90*, 585−606. (h) Que, L., Jr.; True, A. E. *Prog. Inorg. Chem.* **1990**, *38*, 97−200.

(2) (a) Stenkamp, R. E.; Sieker, L. C.; Jensen, L. H. *J. Am. Chem. Soc.* **1984**, *106*, 618−622. (b) Sheriff, S.; Hendrickson, W. A.; Smith, J. L. *J. Mol. Biol.* **1987**, *197*, 273−296. (c) Homes, M. A.; Trong, I. L.; Turley, S.; Sieker, L. C.; Stenkamp, R. E. *J. Mol. Biol.* **1991**, *218*, 583−593.

(3) Nordlund, P.; Sjöberg, B.-M.; Eklund, H. *Nature* **1990**, *345*, 593−598.

(4) Rosenzweig, A. C.; Frederick, C. A.; Lippard, S. J.; Nordlund, P. *Nature* **1993**, *366*, 537−543.

(5) (a) Antanaits, B. C.; Aisen, P. *J. Biol. Chem.* **1982**, *257*, 5330−5332. (b) Antanaits, B. C.; Aisen, P.; Lilienthal, H. R. *J. Biol. Chem.* **1983**, *258*, 3166− 3172.

(6) Averill, B. A.; Davis, J. C.; Burman, S.; Zirino, T.; Sanders-Loehr, J.; Loehr, T. M.; Sage, J. T.; Debrunner, P. G. *J. Am. Chem. Soc.* **1987**, *109*, 3760−3767.

(7) Sinn, E.; O'Connor, C. J.; de Jersey, J.; Zerner, B. *Inorg. Chim. Acta* **1983**, *78*, L13−L15.

(8) (a) Gaber, B. P.; Sheridan, J. P.; Bazer, F. W.; Roberts, R. M. *J. Biol. Chem.* **1979**, *254*, 8340−8342. (b) Antanaits, B. C.; Strekas, T.; Aisen, P. *J. Biol. Chem.* **1982**, *257*, 3766−3770.

(9) (a) True, A. E.; Scarrow, R. C.; Randall, C. R.; Holz, R. C.; Que, L., Jr. *J. Am. Chem. Soc.* **1993**, *115*, 4246−4255. (b) Kauzlarich, S. M.; Teo, B. K.; Zirino, T.; Burman, S.; Davis, J. C.; Averill, B. A. *Inorg. Chem.* **1986**, *25*, 2781−2785. (c) Sjoberg, B.-M.; Graslund, A. *Adv. Inorg. Biochem.* **1983**, *5*, 87− 110.

0020-1669/95/1334-2382$09.00/0

non-heme iron proteins continues to stimulate the synthesis of analogue compounds.

A number of recent model studies focused on the preparation of phenol-containing polypodal ligands having pyridine,[11-18] benzimidazole,[12,19] imidazole,[20-22] and carboxylate pendants. In fact, multidentate ligands are capable of stablizing both Fe^{II}-Fe^{III} and Fe^{III}_2 forms of the complexes and serve as active site models of the PAPs. In particular, we have shown[20] that the polyimidazole ligand 2,6-bis[(bis((1-methylimidazol-2-yl)methyl)amino)methyl]-4-methylphenol (HBIMP) readily stabilizes $Fe^{II}Fe^{III}$ complexes that are good models of the mixed-valence forms of non-heme iron proteins. In addition, HBIMP complexes display the putative axial and rhombic EPR signals with $g_{av} \sim 1.74$, resulting from the antiferromagnetic exchange coupling between high-spin Fe^{II} and Fe^{III} centers, and also display intense phenolate-to-Fe^{III} charge-transfer transitions similar to the transitions observed for PAP proteins. Curiously, there are only a few well-characterized examples of Fe^{III}_2 complexes that contain bridging ligands other than oxide ions[13b,15a,16,17] and only a limited number of diiron complexes that incorporate the biologically relevant imidazole and carboxylate donors.[20-22] In an attempt to prepare new active site models of the oxidized form of purple acid phosphatase, we have synthesized the dinucleating polyimidazole ligand 2,6-bis[((2-hydroxybenzyl)-((1-methylimidazol-2-yl)methyl)amino)methyl]-4-methylphenol (H_3BIOMP) and have found that it readily stabilizes Fe^{III}_2 complexes. Described herein are details of the synthesis of H_3-BIOMP and the crystal structure and magnetic, spectral, and electrochemical properties of a resulting diferric complex.

Experimental Section

All reagents and solvents used in this study were commercially available and were used as received. Solvents were of either reagent or spectroscopic grade and were dried by standard procedures prior to use. 2-(Aminomethyl)-1-methylimidazole dihydrochloride (**1**)[23] and 2,6-bis(chloromethyl)-4-methylphenol (**2**)[11c] were prepared by following previously reported procedures. Elemental analyses were performed by Midwest Analytical, Inc., Indianapolis, IN.

Ligand Syntheses. (a) (2-Hydroxybenzyl)((1-methylimidazol-2-yl)methyl)amine (3). To compound **1** (3.00 g,16.3 mmol) in 150 mL of freshly distilled methanol was added 1.86 g (33 mmol) of KOH under N_2. The reaction mixture was stirred for 1 h and filtered. To the filtrate was added 1.98 g (16.3 mmol) of salicylaldehyde. The resulting yellowish solution was allowed to stir for 2 h, and then 1.80 g (47.3 mmol) of $NaBH_4$ was added. The solution turned colorless immediately, and after 45 min the reaction mixture was quenched by the addition of 1 mL of 5 N HCl. The precipitate was filtered out, and the solvent was removed under vacuum. The crude residue was dissolved in 80 mL of water and extracted with 3 × 40 mL portions of $CHCl_3$. The extracts were combined, washed with brine, and dried with $MgSO_4$. The $CHCl_3$ was then removed under reduced pressure to give 3.25 g (92%) of compound **3**; mp 96 °C. Anal. Calcd for $C_{12}H_{15}N_3O$: C, 66.34; H, 6.96; N, 19.34. Found: C, 66.46; H, 7.01; N, 19.39. ^{1}H NMR ($CDCl_3$, δ): 3.56 (s, 3H), 3.84 (s, 2H), 4.02 (s, 2H), 6.79 (t, 1H), 6.84 (s, 1H), 6.85 (d, 1H), 6.98 (s, 1H), 7.01 (d, 1H), 7.18 (t, 1H). ^{13}C NMR ($CDCl_3$, δ): 32.57 (ImN-*C*H_3), 43.55 (Im-*C*H_2-N), 51.51 (Ph-*C*H_2-N), 116.45 (Ph*C*-H), 119.20 (Ph*C*-H), 121.40 (Im*C*-H), 122.55 (Ph*C*-CH_2), 127.29 (Im*C*-H), 128.92 (Ph*C*-H), 129.02 (Ph*C*-H), 146.15 (Im*C*-CH_2), 157.77 (Ph*C*-OH).

(b) 2,6-Bis[((2-hydroxybenzyl)((1-methylimidazol-2-yl)methyl)-amino)methyl]-4-methylphenol (H_3BIOMP) (4). 2,6-Bis(chloromethyl)-4-methylphenol (**2**) (1.38 g, 6.7 mmol) dissolved in 40 mL of anhydrous tetrahydrofuran was added slowly to a solution containing **3** (2.92 g, 13.4 mmol) and triethylamine (1.42 g, 14.1 mmol) in 120 mL of dry THF under N_2. The resulting solution was allowed to stir for 5 h, and the precipitate was removed by filtration. The filtrate was taken to dryness under reduced pressure, and the crude product was dissolved in 80 mL of $CHCl_3$,and first washed with brine and then with water. The $CHCl_3$ solution was dried with $MgSO_4$ and then taken to dryness under reduced pressure, affording 3.69 g (97% yield) of compound **4**. Anal. Calcd for $C_{33}H_{40}N_6O_4$: C, 67.79; H, 6.89; N, 14.36. Found: C, 67.71; H, 6.86; N, 13.95. ^{1}H NMR ($CDCl_3$, δ): 2.19 (s, 3H), 3.39 (s, 6H), 3.68 (s, 4H), 3.75 (s, 4H), 3.83 (s, 4H), 6.76 (t, 2H), 6.80 (d,2H), 6.81 (s,2H), 6.83 (s, 2H), 7.00 (s, 2H), 7.03 (d, 2H), 7.14 (t, 2H). ^{13}C NMR ($CDCl_3$, δ): 20.45 (Ph-*C*H_3), 32.48 (ImN-*C*H_3), 48.51 (Im-*C*H_2-N), 54.63 (Ph-*C*H_2-N), 56.65 (Ph-*C*H_2-N), 116.61 (Im*C*-H), 118.94 (Im*C*-H), 121.41 (Ph*C*-H), 122.33 (Ph*C*-CH_2), 122.75 (Ph*C*-CH_2), 126.54 (Ph*C*-H), 127.64 (Ph*C*-CH_3), 129.05 (Ph*C*-H), 130.15 (Ph*C*-H), 131.20 (Ph*C*-H), 144.37 (Im*C*-CH_2), 153.87 (Ph*C*-OH), 157.53 (Ph*C*-OH).

Synthesis of $[Fe_2(BIOMP)(\mu\text{-}O_2CCH_3)_2](ClO_4)\cdot H_2O$ (5). To a solution containing 0.608 g (1.1 mmol) of **4** and 0.264 g (3.3 mmol) g of sodium acetate in 20 mL of methanol was added 0.778 g (2.1 mmol) of $Fe(ClO_4)_2\cdot 6H_2O$. The resulting deep purple solution was stirred for 12 h, whereupon a purple precipitate was isolated by filtration. The complex was recrystallized from CH_2Cl_2 by slow diffusion of hexane, yielding 0.652 g (69%) of microcrystalline product. Crystals suitable for X-ray structural analysis were obtained by vapor diffusion of ether into a CH_3CN/propanol (3:1) solution of the complex. Anal. Calcd for $Fe_2C_{37}H_{41}N_6ClO_{11}$: C, 49.77; H, 4.63; N, 9.41. Found: C, 49.48; H, 4.70; N, 9.47. Electronic spectral data (acetonitrile, λ_{max} (nm), ϵ_M (M^{-1} cm^{-1})): 586 (7400), 336 (7650), 276 (20 800), 222 (29 300). Electronic spectral data (methanol, λ_{max} (nm), ϵ_M (M^{-1} cm^{-1})): 536 (5120), 328 (9880), 280 (17 800), 222 (30 700).

Caution! Perchlorate salts of metal complexes are potentially explosive and should be handled in small quantities with care.

Physical Measurements. UV−visible spectra were recorded using a Hewlett Packard HP8452A diode-array spectrophotometer. ^{1}H and

(10) (a) Lauffer, R. B.; Antanaits, B. C.; Aisen, P.; Que, L., Jr. *J. Biol. Chem.* **1983**, *258*, 14212−14218. (b) Scarrow, R. C.; Pyrz, J. W.; Que, L., Jr. *J. Am. Chem. Soc.* **1990**, *112*, 657−665.

(11) (a) Borovik, A. S.; Hendrich, M. P.; Holman, T. R.; Münck, E.; Papaefthymiou, V.; Que, L., Jr. *J. Am. Chem. Soc.* **1990**, *112*, 6031−6038. (b) Borovik, A. S.; Papaefthymiou, V.; Taylor, L. F.; Anderson, O. P.; Que, L., Jr. *J. Am. Chem. Soc.* **1989**, *111*, 6183−6195. (c) Borovik, A. S.; Que, L., Jr. *J. Am. Chem. Soc.* **1988**, *110*, 2345−2347. (d) Schepers, K.; Bremer, B.; Krebs, B.; Henkel, G.; Althaus, E.; Mosel,B.; Müller-Warmuth, W. *Angew. Chem.* **1990**, *102*, 582−584; *Angew. Chem., Int. Ed. Engl.* **1990**, *29*, 531−533.

(12) (a) Suzuki, M.; Oshio, H.; Uehara, A.; Endo, K.; Yanaga, M.; Kida, S.; Saito, K. *Bull. Chem. Soc. Jpn.* **1988**, *61*, 3907−3913. (b) Suzuki, M.; Uehara, A.; Oshio, H.; Endo, K.; Yanaga, M.; Kida, S.; Saito, K. *Bull. Chem. Soc. Jpn.* **1987**, *60*, 3547−3555. (c) Suzuki, M.; Kanatomi, H.; Murase, I. *Chem. Lett., Chem. Soc. Jpn.* **1981**, 1745−1748.

(13) (a) Borovik, A. S.; Murch, B. P.; Que, L., Jr.; Papaefthymiou, V.; Münck, E. *J. Am. Chem. Soc.* **1987**, *109*, 7190−7191. (b) Murch, B. P.; Bradley, F. C.; Que, L., Jr. *J. Am. Chem. Soc.* **1986**, *108*, 5027−5028.

(14) Yan, S.; Que, L., Jr. *J. Am. Chem. Soc.* **1988**, *110*, 5222−5224.

(15) (a) Neves, A.; de Brito, M. A.; Vencato, I.; Drago, V.; Griesar, K.; Haase, W.; Wascarenhas, Y. P. *Inorg. Chim. Acta* **1993**, *214*, 5−8. (b) Neves, A.; Erthal, S. M. D.; Drago, V.; Griesar, K.; Haase, W. *Inorg. Chim. Acta* **1992**, *197*, 121−124.

(16) Krebs, B.; Schepers, K.; Bremer, B.; Henkel, G.; Althaus, E.; Müller-Warmuth, W.; Griesar, K.; Haase, W. *Inorg. Chem.* **1994**, *33*, 1907−1914.

(17) Campbell, V. D.; Parsons, E. J.; Pennington, W. T. *Inorg. Chem.* **1993**, *32*, 1773−1778.

(18) Bernard, E.; Moneta, W.; Laugier, J.; Chardon-Noblat, S.; Deronzier, A.; Tuchagues, J.-P.; Latour, J.-T. *Angew. Chem., Int. Ed. Engl.* **1994**, *33*, 887−889.

(19) (a) Suzuki, M.; Uehara, A.; Endo, K. *Inorg. Chim. Acta* **1986**, *123*, L9−L10. (b) Suzuki, M.; Murata, S.; Uehara, A.; Kida, S. *Chem. Lett., Chem. Soc. Jpn.* **1987**, 281−284.

(20) (a) Mashuta, M. S.; Webb, R. J.; McCusker, J. K.; Schmitt, E. A.; Oberhausen, K. J.; Richardson, J. F.; Buchanan, R. M.; Hendrickson, D. N. *J. Am. Chem. Soc.* **1992**, *114*, 3815−3827. (b) Mashuta, M. S.; Webb, R. J.; Oberhausen, K. J.; Richardson, J. F.; Buchanan, R. M.; Hendrickson, D. N. *J. Am. Chem. Soc.* **1989**, *111*, 2745−2746.

(21) Tolman, W. B.; Liu, S.; Bensten, J. G.; Lippard, S. J. *J. Am. Chem. Soc.* **1991**, *113*, 152−164.

(22) Stassinopoulos, A.; Schulte, G.; Papaefthymiou, G. C.; Caradonna, J. P. *J. Am. Chem. Soc.* **1991**, *113*, 8686−8697.

(23) Oberhausen, K. J.; Richardson, J. F.; Pierce, W.; Buchanan, R. M. *Polyhedron* **1989**, *8*, 659−668.

Table 1. Crystallographic Data for $[Fe_2(BIOMP)(O_2CCH_3)_2]ClO_4 \cdot H_2O$ (**5**)

formula	$Fe_2C_{37}H_{43}N_6ClO_{12}$	ϱ_{calc}, g/cm^3	1.53
fw	910.93	ϱ_{obs}, g/cm^3	1.53(1)
a, Å	14.983(14)	radiation (λ, Å)	Mo Kα (0.710 73)
b, Å	12.341(13)	temp, K	295(1)
c, Å	21.391(16)	abs coeff, cm^{-1}	8.71
β, deg	90.79(7)	R^a	0.067
V, Å^3	3955(6)	$R_w{}^b$	0.083
Z	4	GOF	2.83
space group	$P2_1/n$ (No. 14)		

$^a R = \sum(||F_o| - |F_c||)/\sum|F_o|$. $^b R_w = [\sum w(|F_o| - |F_c|)^2/\sum w|F_o|^2]^{1/2}$; $w = 1/\sigma^2(F_o)$.

^{13}C NMR spectra were obtained using a Varian XL-300 spectrometer. Electrochemical measurements were obtained using dried and degassed acetonitrile solutions of compound **5** containing 0.1 M tetra-*n*-butylammonium perchlorate. Cyclic voltammograms were obtained using a PAR Model 175 universal Programmer, a PAR Model 173/178 potentiostat, and a digital coulometer interfaced with a Houston Model 2000 X-Y recorder. A conventional three-electrode cell, utilizing Ag/AgCl reference and platium wire and coil working electrodes, was used for all measurements. Redox potentials are referenced relative to an external ferrocene/ferrocenium standard ($E_{1/2}$ = 0.500 V vs Ag/AgCl). D.c. magnetic susceptibility measurements were carried out on a Quantum Design MPMS5 SQUID susceptometer equipped with a 55 kG magnet and operating in the range 1.8−400 K. Pascal's constants were used to estimate the diamagnetic corrections and were subtracted from the experimental susceptibilities to give the molar paramagnetic susceptibilities. Variable-temperature ^{57}Fe Mössbauer spectra were obtained using a constant-acceleration spectrometer described elsewhere.[24] Isomer shift values are reported relative to Fe foil at 300 K and have not been corrected for the temperature-dependent second-order Doppler shift.

X-ray Data Collection and Reduction. A purple block-shaped crystal of $[Fe_2(BIOMP)(O_2CCH_3)_2]ClO_4 \cdot H_2O$ (**5**) of dimensions 0.35 × 0.25 × 0.25 mm was mounted on a glass fiber and coated with epoxy. X-ray intensity data were collected using an Enraf-Nonius CAD-4 diffractometer equipped with a graphite monochromator (Mo Kα radiation, λ = 0.710 73 Å). A summary of pertinent crystallographic data is given in Table 1. Cell constants and an orientation matrix for data collection were obtained from a least-squares refinement using the setting angles of 25 carefully centered reflections in the range $30° < 2\theta < 36°$. Data were collected at 22(1) °C using the ω-2θ scan technique to a maximum 2θ value of 46.0°. The intensities of three standard reflections were monitored every 60 min, and a linear decay of 4.1% was applied. Of the 7309 reflections measured, 5807 were found to be unique (R_{int} = 0.132); 3493 reflections were considered observed with $I > 3.0\sigma(I)$. Intensity data were corrected for Lorentz and polarization effects, and an empirical absorption correction (DIFABS[25]) was applied which resulted in transmission factors ranging from 0.86 to 1.20.

Structure Solution and Refinement. The structure was solved by Patterson and refined by direct methods (DIRDIF[26]). Atomic positional and isotropic thermal parameters for all non-hydrogen atoms are given in Table 2. All non-hydrogen atoms, except those having occupancies less than 1, were refined anisotropically using full-matrix least-squares methods. The function minimized was $\sum w(|F_o| - |F_c|)^2$. Hydrogen atoms were included as fixed contributions (B_{iso} = 1.2B_{iso} of attached carbon atom) in calculated positions. The perchlorate counterion was found to be positionally disordered. This was modeled using two separate ClO′$_2$ fragments and two common oxygen atoms. O9ab and O10ab were both assigned occupancy factors of 1.0 and refined anisotropically. The disordered chlorine and two remaining oxygen atoms of each fragment were assigned different occupancy factors. One set of disordered atoms were given occupancy factors of $^2/_3$ each and refined anisotropically, while the atoms of the second fragment were given occupancies of $^1/_3$ each and refined isotropically. A total of 536 parameters were refined in the final cycles of least squares (R = 0.067 and R_w = 0.083). Atom scattering factors were taken from Cromer and Waber[27] and the values for $\Delta f'$ and $\Delta f''$ were those of Creagh

Table 2. Atomic Coordinates and B_{eq} Values for Compound **5**

atom	x	y	z	B_{eq},^{a} Å^2
Fe(1)	0.35230(10)	0.6128(1)	0.29341(7)	2.26(4)
Fe(2)	0.5241(1)	0.5839(1)	0.18066(7)	2.30(3)
Cl(1)	0.563(1)	0.258(2)	0.4020(8)	6.6(4)
Cl(2)	0.560(3)	0.234(4)	0.397(2)	5.3(7)
O(1)	0.4819(4)	0.6492(5)	0.2652(3)	2.3(2)
O(2)	0.2407(4)	0.5765(6)	0.3264(3)	3.0(2)
O(3)	0.5634(5)	0.5376(6)	0.1022(3)	3.4(2)
O(4)	0.3776(5)	0.4544(6)	0.2788(4)	3.3(2)
O(5)	0.4741(5)	0.4403(6)	0.2010(4)	3.7(2)
O(6)	0.3031(5)	0.6455(6)	0.2082(3)	3.1(2)
O(7)	0.4140(5)	0.6545(6)	0.1411(3)	3.0(2)
O(8)	0.5553(8)	0.2830(9)	0.0879(5)	8.5(4)
O(9ab)	0.4873(9)	0.248(1)	0.4366(6)	12.2(5)
O(10ab)	0.548(1)	0.305(1)	0.3478(7)	14.1(6)
O(11a)	0.632(2)	0.337(2)	0.4225(10)	13.8(10)
O(11b)	0.525(3)	0.149(3)	0.357(2)	8(1)
O(12a)	0.611(2)	0.164(2)	0.408(2)	18(1)
O(12b)	0.636(3)	0.215(3)	0.430(1)	4.5(7)
N(1)	0.4057(5)	0.6069(6)	0.3906(4)	2.1(2)
N(2)	0.3430(6)	0.7768(7)	0.3176(4)	2.6(2)
N(3)	0.3847(6)	0.9042(7)	0.3848(4)	3.4(2)
N(4)	0.5987(5)	0.7380(6)	0.1640(4)	2.2(2)
N(5)	0.6428(5)	0.5555(7)	0.2299(4)	2.6(2)
N(6)	0.7633(6)	0.6294(8)	0.2730(4)	3.2(2)
C(1)	0.5364(6)	0.7128(8)	0.3001(5)	2.0(2)
C(2)	0.5498(6)	0.6920(8)	0.3625(5)	1.9(2)
C(3)	0.6048(8)	0.7566(10)	0.3968(5)	3.3(3)
C(4)	0.6496(7)	0.8475(10)	0.3733(5)	3.2(3)
C(5)	0.6334(7)	0.8662(8)	0.3099(5)	2.9(3)
C(6)	0.5784(6)	0.8033(8)	0.2734(5)	2.1(2)
C(7)	0.7097(9)	0.916(1)	0.4109(6)	5.0(4)
C(8)	0.5031(7)	0.5952(8)	0.3905(5)	2.5(2)
C(9)	0.3697(8)	0.5106(9)	0.4242(5)	3.0(3)
C(10)	0.2702(8)	0.5064(9)	0.4302(5)	2.8(3)
C(11)	0.2133(8)	0.5337(9)	0.3820(6)	3.4(3)
C(12)	0.1172(8)	0.5200(10)	0.3866(6)	4.1(3)
C(13)	0.089(1)	0.474(1)	0.4444(8)	6.0(4)
C(14)	0.1464(10)	0.449(1)	0.4931(6)	4.5(4)
C(15)	0.2334(8)	0.4638(9)	0.4837(6)	3.8(3)
C(16)	0.3823(8)	0.7103(9)	0.4245(5)	3.1(3)
C(17)	0.3722(7)	0.7971(8)	0.3759(5)	2.5(3)
C(18)	0.3384(7)	0.8766(9)	0.2875(5)	3.1(3)
C(19)	0.3612(9)	0.9523(9)	0.3275(6)	4.1(3)
C(20)	0.4140(10)	0.9566(10)	0.4415(6)	5.4(4)
C(21)	0.5634(8)	0.8252(8)	0.2056(5)	2.8(3)
C(22)	0.5827(7)	0.7748(8)	0.0980(5)	2.9(3)
C(23)	0.6122(7)	0.6976(8)	0.0477(5)	2.4(3)
C(24)	0.5950(7)	0.5867(9)	0.0507(5)	2.6(3)
C(25)	0.6143(8)	0.5212(9)	−0.0023(5)	3.4(3)
C(26)	0.6472(8)	0.567(1)	−0.0553(5)	3.6(3)
C(27)	0.6642(8)	0.676(1)	−0.0584(5)	3.7(3)
C(28)	0.6464(8)	0.7412(9)	−0.0075(5)	3.5(3)
C(29)	0.6953(7)	0.7181(8)	0.1764(5)	2.8(3)
C(30)	0.7037(7)	0.6346(9)	0.2266(5)	2.8(3)
C(31)	0.6671(8)	0.4976(9)	0.2826(5)	3.2(3)
C(32)	0.7408(9)	0.5417(10)	0.3093(5)	3.7(3)
C(33)	0.8398(9)	0.701(1)	0.2858(7)	5.9(4)
C(34)	0.4193(7)	0.3988(9)	0.2388(5)	2.9(3)
C(35)	0.4033(8)	0.2805(9)	0.2361(5)	3.7(3)
C(36)	0.3343(8)	0.6709(8)	0.1554(5)	2.7(3)
C(37)	0.2721(9)	0.719(1)	0.1096(6)	4.5(3)

$^a B_{eq} = {}^8/_3\pi^2(U_{11}(aa^*)^2 + U_{22}(bb^*)^2 + U_{33}(cc^*)^2 + 2U_{12}aa^*bb^* \cos\gamma + 2U_{13}aa^*cc^* \cos\beta + 2U_{23}bb^*cc^* \cos\alpha)$.

(24) Cohn, M. J.; Timken, M. D.; Hendrickson, D. N. *J. Am. Chem. Soc.* **1984**, *106*, 6683−6689.
(25) Walker, N.; Stuart, D. *Acta Crystallogr.* **1983**, *A39*, 158−166.
(26) Beurskens, P. T.; Admiraal, G.; Beurskens, G.; Bosman, W. P.; Garcia-Granda, S.; Gould, R. O.; Smits, J. M. M.; Smykalla, C. The DIRDIF program system, Technical Report of the Crystallography Laboratory, University of Nijmegen, The Netherlands, 1992.
(27) Cromer, D. T.; Waber, J. T. *International Tables for X-ray Crystallography*; Kynoch Press: Birmingham, England, 1974; Vol. IV, Table 2.2 A.

Scheme 1

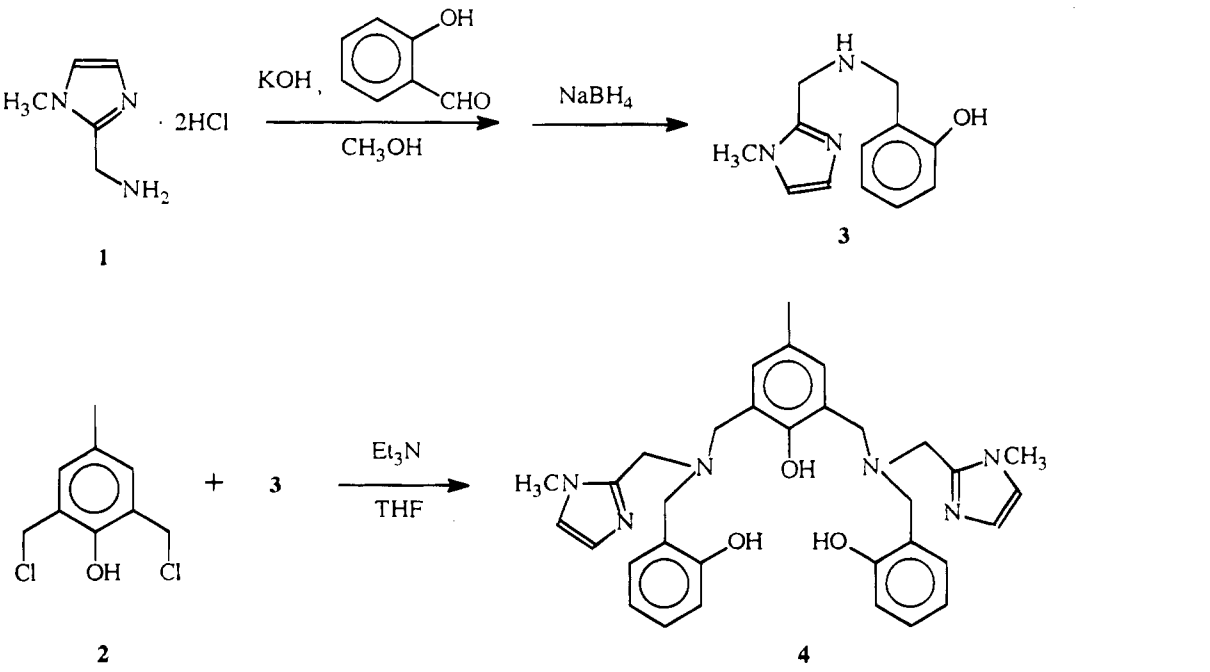

and McAuley.[28] All calculations were performed using the teXsan crystallographic software package.[29]

Results and Discussion

Synthesis. The ligand H_3BIOMP has been synthesized by reacting 2,6-bis(chloromethyl)-*p*-cresol (**2**) with (2-hydroxybenzyl)((1-methylimidazol-2-yl)methyl)amine (**3**) in THF containing a slight excess of triethylamine (Scheme 1). The structure and purity of compound **4** were confirmed by ^{1}H and ^{13}C NMR as well as by elemental analyses.

A diferric complex of the ligand is readily prepared by addition of 2 equiv of $Fe(ClO_4)_2{\cdot}6H_2O$ to a methanol solution containing H_3BIOMP and 3 equiv of the appropriate sodium carboxylate salt in air. When the reaction was conducted under an inert atmosphere (Ar), a pale red-purple solution was detected upon mixing. The color of the solution persisted for several hours in nearly oxygen-free solutions. The optical spectrum of the complex is consistent with the partially oxidized mixed-valence $Fe^{III}Fe^{II}$ form of the complex, formed due to low levels of O_2 present in solution. Unfortunately, we have not been able to isolate a pure form of this complex under these reaction conditions. Efforts to isolate the mixed-valence complex by both chemical and electrochemical reduction are in progress.

Brief exposure of the initial red-purple solution to air results in immediate oxidation of the intermediate to compound **5**. The resulting purple complex precipitated from the reaction mixture and was isolated by filtration and recrystallized by vapor diffusion of ether into an acetonitrile/propanol (3:1) solution of the complex.

X-ray Crystal Structure of $[Fe_2(BIOMP)(O_2CCH_3)_2]$-$ClO_4{\cdot}H_2O$ (5). The structure of compound **5** is shown in Figure 1, and selected bond lengths and bond angles are given in Table 3. Both Fe^{III} centers are triply bridged by an oxygen atom from a phenolate and two acetate ions and have distorted octahedral geometries. The remaining facial coordination sites of each iron center are occupied by a phenolate oxygen atom and nitrogen

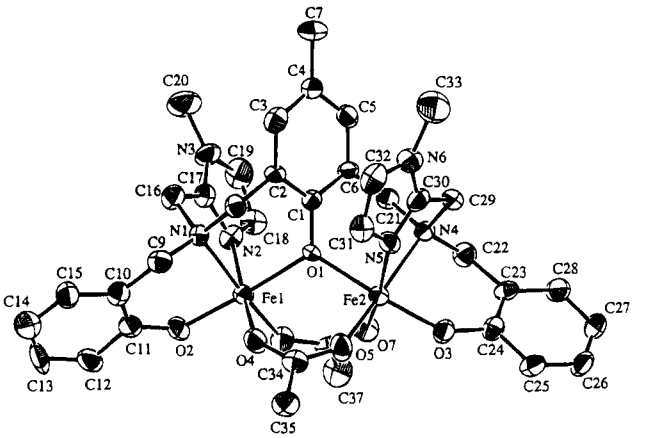

Figure 1. ORTEP view (50% probability ellipsoids) of compound **5** with labeling scheme.

atoms from amine and imidazole pendants. The two terminal phenol pendants of the trianionic $BIOMP^{3-}$ ligand are bonded trans to the bridging phenolate group, resulting in approximate C_2 symmetry for the cation. A similar structure has been reported for a related Fe^{III}_2 complex containing the ligand H_3-BBPMP.[15a] The Fe(1)−O(1)−Fe(2) bridging angle in **5** is 117.5(3)°, somewhat smaller than the angle of 118.3(4)° reported for $[Fe_2(BBPMP)(O_2CCH_3)_2]^{2+}$.[15a] In addition, the Fe−Fe separation of 3.567(3) Å in **5** is slightly longer than the values of 3.442(2) and 3.528(8) Å reported for $[Fe_2(HXTA)$-$(O_2CCH_3)_2]^-$ [13b] and $[Fe_2(BBPMP)(O_2CCH_3)_2]^{2+}$,[15a] respectively, and is significantly shorter than the 3.837(8) Å separation reported for $[Fe_2BHPMP(O_2P(OPh)_2)_2]^+$.[16]

The Fe(1)−O(1) and Fe(2)−O(1) bond distances in **5** are 2.091(7) and 2.086(6) Å, respectively, significantly longer than the Fe^{III}−O (phenolate) lengths of 1.958(2) and 1.943(2) Å reported for $[Fe^{II}Fe^{III}(BIMP)(O_2CC_6H_5)_2]^{2+}$ [20] and $[Fe^{II}Fe^{III}$-$(BPMP)(O_2CCH_2CH_3)_2]^{2+}$ [11b,c] and lengths of 2.035(3), 2.055(8), and 2.008(2) Å observed for $[Fe^{III}Mn^{II}(BIMP)(O_2CCH_3)_2]^{2+}$,[30] $[Fe_2(BBPMP)(O_2CCH_3)_2]^+$,[15a] and $[Fe_2(HXTA)(O_2CCH_3)_2]^-$,[13b] respectively. The terminal Fe^{III}−O(phenolate) bond lengths in **5** (Fe(1)−O(2) = 1.878(7) Å and Fe(2)−O(3) = 1.876(7) Å)

(28) Creagh, D. C.; McAuley, W. J. *International Tables for X-ray Crystallography*; Wilson, A. J. C., Ed.; Kluwer Academic Publishers: Boston, MA, 1992; Vol. C, Table 4.2.6.8, pp 219−222.
(29) *teXsan: Single Crystal Structure Analysis Software*, version 1.6; Molecular Structure Corp.: The Woodlands, TX 77381, 1993.

Table 3. Selected Bond Lengths (Å) and Angles (deg) for Compound **5**

	Bond Lengths		
Fe(1)−Fe(2)	3.567(3)		
Fe(1)−O(1)	2.091(7)	Fe(2)−O(1)	2.086(6)
Fe(1)−O(2)	1.878(7)	Fe(2)−O(3)	1.876(7)
Fe(1)−O(4)	2.016(8)	Fe(2)−O(5)	1.974(7)
Fe(1)−O(6)	1.999(7)	Fe(2)−O(7)	2.040(7)
Fe(1)−N(1)	2.219(8)	Fe(2)−N(4)	2.238(8)
Fe(1)−N(2)	2.094(9)	Fe(2)−N(5)	2.085(9)
	Bond Angles		
O(1)−Fe(1)−O(2)	174.4(3)	O(1)−Fe(2)−O(5)	92.0(3)
O(1)−Fe(1)−O(6)	91.4(3)	O(1)−Fe(2)−N(4)	88.1(3)
O(1)−Fe(1)−N(2)	85.9(3)	O(3)−Fe(2)−O(5)	92.8(3)
O(2)−Fe(1)−O(6)	94.2(3)	O(3)−Fe(2)−N(4)	87.3(3)
O(2)−Fe(1)−N(2)	94.3(3)	O(5)−Fe(2)−O(7)	99.7(3)
O(4)−Fe(1)−N(1)	92.7(3)	O(5)−Fe(2)−N(5)	93.5(3)
O(6)−Fe(1)−N(1)	170.2(3)	O(7)−Fe(2)−N(5)	164.0(3)
N(1)−Fe(1)−N(2)	79.9(3)	O(1)−Fe(2)−O(3)	175.0(3)
O(1)−Fe(1)−O(4)	89.2(3)	O(1)−Fe(2)−O(7)	86.6(3)
O(1)−Fe(1)−N(1)	87.3(3)	O(1)−Fe(2)−N(5)	83.9(3)
O(2)−Fe(1)−O(4)	89.8(3)	O(3)−Fe(2)−O(7)	91.2(3)
O(4)−Fe(1)−O(6)	97.0(3)	O(5)−Fe(2)−N(4)	171.9(3)
O(4)−Fe(1)−N(2)	171.3(3)	O(7)−Fe(2)−N(4)	88.5(3)
O(6)−Fe(1)−N(2)	90.3(3)	N(4)−Fe(2)−N(5)	78.4(3)
Fe(1)−O(1)−Fe(2)	117.5(3)		

are much shorter than the corresponding Fe^{III}−O bond lengths of 1.924(6) and 1.931(7) Å in $[Fe_2L_2O(O_2CC_6H_5)]^+$ (L = (2-hydroxybenzyl)-bis(2-pyridylmethyl)amine.[14] The Fe−N(amine) bond distances average to a value of 2.229(8) Å, while the Fe−N(imidazole) lengths average to 2.089(8) Å. As with the $[Fe_2(BIMP)(O_2CC_6H_5)_2]^{2+}$ and $[FeMn(BIMP)(O_2CCH_3)_2]^{2+}$ cations, the N−Fe−N chelate angles in **5** are <90° (N(1)−Fe(1)−N(2) = 79.9(3)°, and N(4)−Fe(2)−N(5) = 78.4(3)°). The remaining bond angles within the coordination sphere also deviate substantially from those expected for octahedral geometry.

Magnetic Susceptibility and Mössbauer Studies. Variable-temperature d.c. magnetic susceptibility data were collected on a dried sample of $[Fe_2(BIOMP)(O_2CCH_3)_2]ClO_4$ in a 10 kG field. A plot of the effective magnetic moment per dinuclear complex in the range 2.0−320.0 K is shown in Figure 2. The two high-spin Fe^{III} centers are weakly coupled antiferromagnetically. The effective magnetic moment (μ_{eff}) per Fe^{III}_2 decreases gradually from 7.61 μ_B at 300 K and then rapidly to 0.351 μ_B at 2.00 K (Figure 2). The data were least-squares-fitted to the Hamiltonian in eq 1. In eq 1 the first term is the

$$\hat{H} = -2J\vec{S}_1\cdot\vec{S}_2 + g\mu_B H_z S_z + D[S_{z^2} - S(S+1)/3] \quad (1)$$

isotropic Heisenberg exchange interaction, the second term is an isotropic Zeeman interaction, and the third term is the axial single-ion zero-field splitting. Using the computer program DIMER,[31] the Hamiltonian matrix was constructed with a set of uncoupled product basic functions. The eigenvalues and eigenvectors were evaluated on each least-squares cycle by diagonalizing a 36 × 36 Hamiltonian matrix. The paramagnetic susceptibility χ of the dimer was then obtained from the calculated magnetization using eq 2, where the derivatives of

$$M = \chi H = N\sum_{i=1}^{p}(-\delta E_i/\delta H)\exp(-E_i/kT)/\sum_{i=1}^{p}\exp(-E_i/kT) \quad (2)$$

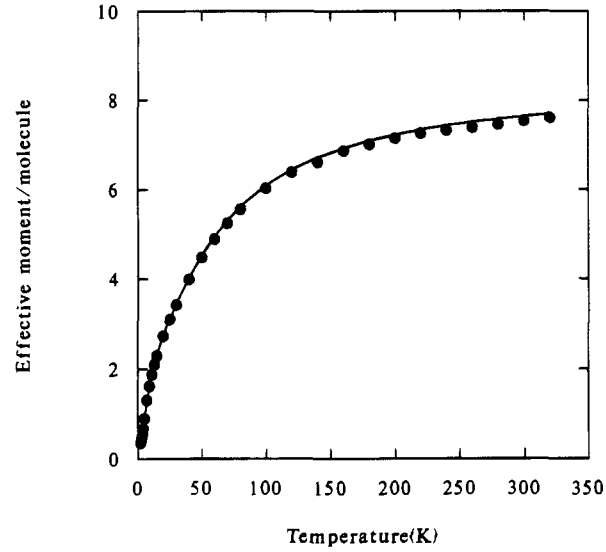

Figure 2. Plot of the effective magnetic moment per dinuclear complex vs temperature for compound **5**. The solid line resulted from a least-squares fit of the data.

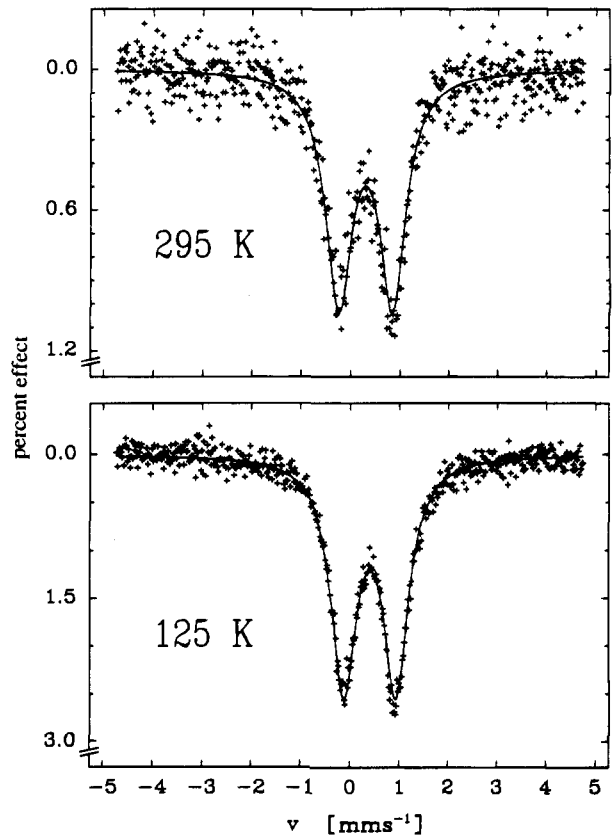

Figure 3. ^{57}Fe Mössbauer spectra for a polycrystalline sample of compound **5** at 125 and 295 K. Each spectrum was least-squares-fit to Lorentzian line shapes corresponding to one quadrupole-split doublet.

energy of each level with respect to the magnetic field ($\delta E_i/\delta H$) were calculated by evaluating slopes. Least-squares fitting was used to fit the temperature dependence of the magnetic moment as a function of temperature. The parameters J (magnetic exchange), D (single-ion zero-field splitting), and an isotropic g value were evaluated.

A good fit for the data, μ_{eff} per Fe_2 vs T, was found when $J = -6.4$ cm^{-1}, $D = 0.0$ cm^{-1}, and $g = 2.00$. The temperature-independent paramagnetism (TIP) was held fixed at 400 × 10^{-6} cgsu, and in order to accommodate the lowest-temperature data, a paramagnetic impurity of 0.13% weight of a monomeric Fe^{3+}

(30) Buchanan, R. M.; Mashuta, M. S.; Richardson, J. F.; Webb, R. J.; Oberhausen, K J.; Nanny, M. A.; Hendrickson, D. N. *Inorg. Chem.* **1990**, *29*, 1299−1301.
(31) Schmitt, E. A.; Hendrickson, D. N. Unpublished results.

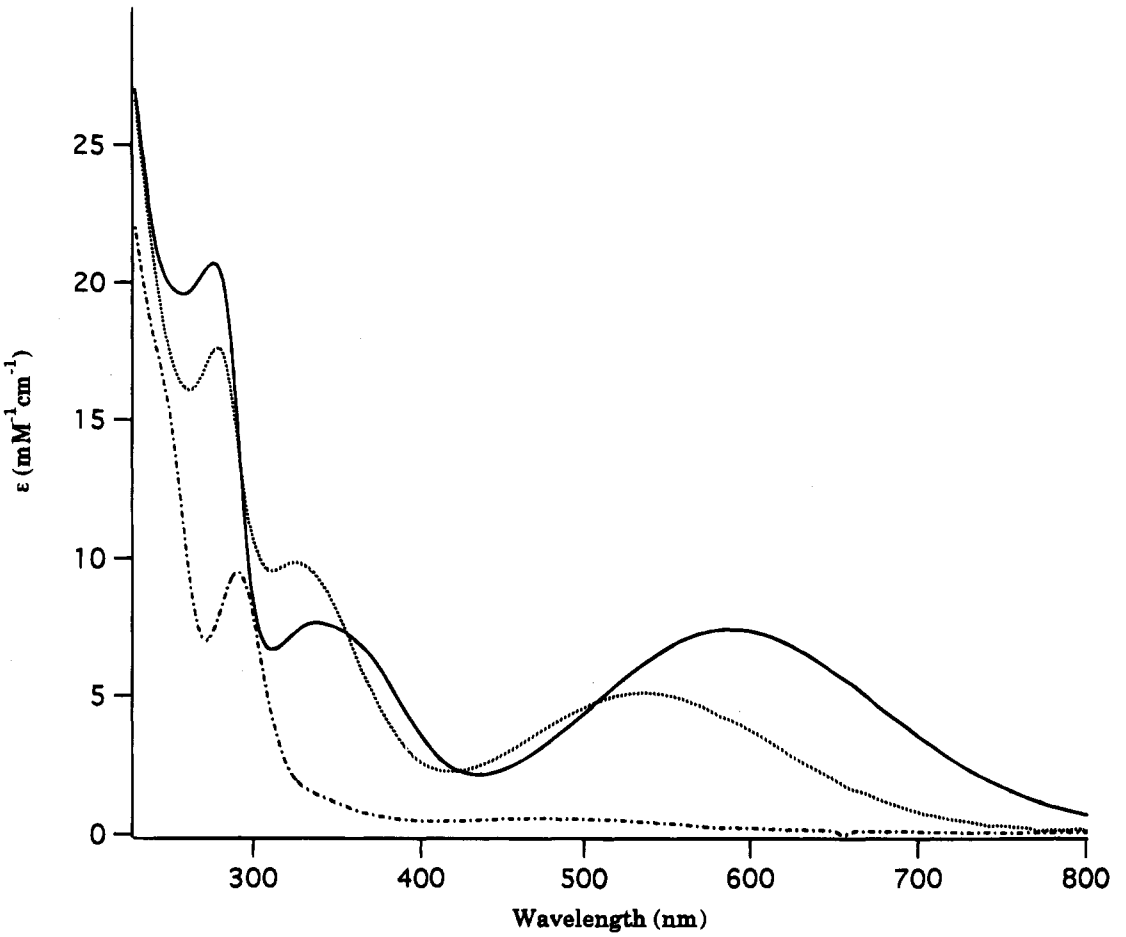

Figure 4. Electronic spectra for the initial intermediate in methanol under Ar (— · —) and compound **5** in CH_3CN (—) and methanol (···).

was included. Previously reported μ-phenoxo-bridged ferric dimers have been shown to have magnetic exchange parameters ranging from -5.6 cm^{-1} for $[Fe_2BHPMP(O_2P(OPh)_2)_2]ClO_4 \cdot H_2O$[16] to -12 cm^{-1} for $[Fe_2BPMP(C_6H_5CO_2)](ClO_4)_3 \cdot CH_3CN \cdot H_2O$;[12a] PAP_o has been reported to have $J \sim -40$ to -150 cm^{-1}.[1e,f,h] Complex **5** most closely resembles the former complex which was reported to have a weaker antiferromagnetic interaction ($J = -5.6$ cm^{-1}) as a direct consequence of the larger Fe—O(bridge) bond length and the result of trans influence of the phenolate oxygens. This argument also holds for the structurally similar complex **5** which has an average Fe—O(phenolate) bond length of 1.87 Å and is trans to the Fe—O(bridge) bond (average 2.08 Å).

^{57}Fe Mössbauer spectra of **5** were recorded at 295 and at 125 K (Figure 3). Both spectra display a single quadrupole-split doublet, consistent with a high-spin octahedral Fe^{III}_2 complex. The quadrupole splitting (ΔE_Q) is equal to 1.083(23) mm/s at 295 K and 1.055(9) mm/s at 125 K. The isomer shift (δ) parameters at 295 and 125 K are 0.406(13) and 0.508(5) mm/s, respectively.

Electronic Absorption Spectra of 5. The UV—vis spectra of compound **5** in both methanol and acetonitrile as well as the spectrum of the initial red-purple intermediate in methanol are displayed in Figure 4. As previously noted, during the initial stages of the reaction, we observed the formation of a pale red-purple intermediate that displays an optical spectrum consistent with previously reported mixed-valence $Fe^{II}Fe^{III}$ complexes. Transitions are observed for this intermediate at 290 nm (ϵ = 9600 M^{-1} cm^{-1}/Fe$_2$), 330 nm (ϵ = 1650 M^{-1} cm^{-1}/Fe$_2$), and 494 nm (ϵ = 550 M^{-1} cm^{-1}/Fe$_2$). Exposure of solutions containing the red-purple intermediate to air results in its immediate oxidation to compound **5**. The spectrum of **5** in methanol is noticeably blue shifted compared to the spectrum of the complex in acetonitrile. In acetonitrile the complex exhibits spectral features at 276 nm (ϵ = 20 800 M^{-1} cm^{-1}/Fe$_2$), 336 nm (ϵ = 7650 M^{-1} cm^{-1}/Fe$_2$), and 586 nm (ϵ = 7400 M^{-1} cm^{-1}/Fe$_2$), while in methanol transitions are observed at 280 nm (ϵ = 17 800 M^{-1} cm^{-1}/Fe$_2$), 328 nm (ϵ = 9880 M^{-1} cm^{-1}/Fe$_2$), and 536 nm (ϵ = 5120 M^{-1} cm^{-1}/Fe$_2$). The bands at 494, 586, and 536 nm are associated with phenolate-to-Fe^{III} charge-transfer transitions involving both terminal and bridging phenolate groups. The extinction coefficient associated with this charge transfer transition in **5** is larger than those reported for most synthetic Fe^{III}—phenolate complexes[11,12,13b,20] and mixed-valence $Fe^{II}Fe^{III}$ complexes[11b,c,20] but is comparable to values reported for the related compounds $[Fe_2(HDP)_2O(O_2CC_6H_5)]^+$ (HDP = (2-hydroxybenzyl)bis(2-pyridylmethyl)-amine)[14] and $[Fe_2(BBPMP)(O_2CCH_3)_2]^+$,[15a] as well as for PAP_o (ϵ = 4000 M^{-1} cm^{-1}).[6,7] The phenolate-to-Fe^{III} charge-transfer transition associated with the intermediate is comparable in magnitude to those reported for $Fe^{II}Fe^{III}$ complexes. The higher energy transitions in the spectra of **5** and the red-purple intermediate are also attributed to ligand-to-metal and intraligand charge-transfer transitions.

Electrochemistry. The electrochemical properties of compound **5** have been evaluated by cyclic voltammetry. A cyclic voltammogram of the complex in acetonitrile containing 0.1 M TBAP is shown in Figure 5. The complex displays two quasireversible redox processes corresponding to the $Fe^{II}_2/Fe^{II}Fe^{III}$ and $Fe^{II}Fe^{III}/Fe^{III}_2$ forms of the complex at -0.785 and -0.225 V vs Ag/AgCl, respectively. The peak-to-peak separation (ΔE) of the $Fe^{III}_2/Fe^{II}Fe^{III}$ couple is 0.075 V and was found to be independent of scan rate between 10 and 100 mV/s. The $Fe^{III}Fe^{II}/Fe^{II}_2$ redox couple, however, has a peak-to-peak separa-

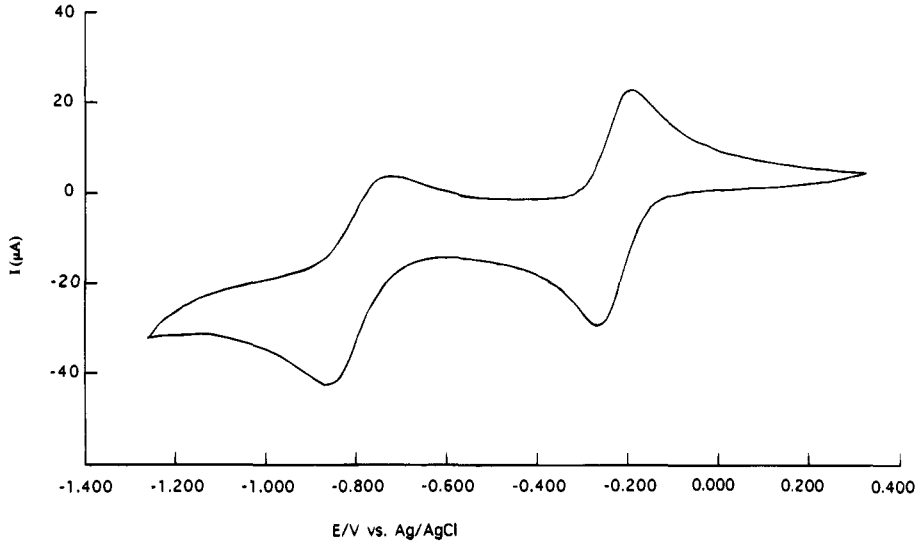

Figure 5. Cyclic voltammogram of compound **5** in CH_3CN (0.1 M TBAP as a supporting electrolyte) at a glassy-carbon electrode. The reference electrode was a Ag/AgCl electrode and the scan rate was 10 mV/s.

tion of $\Delta E = 0.119$ V and is also independent of the scan rate between 10 and 100 mV/s. Both redox couples have i_{pc}/i_{pa} ratios close to unity at a scan rate of 50 mV/s.

We have determined the stability of the $Fe^{II}Fe^{III}$ mixed-valence form of the complex by evaluating its comproportionation constant ($\ln K_{com} = (E^\circ_2 - E^\circ_1)F/RT$). From the separation of the two redox processes, we have determined K_{com} to be 4.3 $\times$ 10^9 M^{-1}, indicating that the mixed-valence complex is stabilized by the $BIOMP^{3-}$ ligand. However the negative redox potentials associated with formation of the Fe^{II}_2 and $Fe^{II}Fe^{III}$ forms of compound **5** and their sensitivity to the presence of low levels of O_2 in solution have led to difficulties in isolating pure forms of these complexes.

Two quasireversible one-electron redox processes have been reported to occur at -1.15 and -0.57 V vs Fc^+/Fc for the related complex $[Fe_2(BBPMP)(O_2CCH_3)_2]^{n+}$.[15a] Unfortunately, the values reported in the text by Neves et al. do not agree with those extracted directly from the voltammogram. Correcting the data to conform to a Ag/AgCl reference electrode gives values of -0.84 and -0.29 V for the two redox processes. These values are similar to those observed for compound **5**.

In both cases, the redox processes are significantly shifted to more cathodic potentials compared to those of other phenolate-bridged diiron complexes. For instance, the redox potentials of $[Fe_2(BZIM)(O_2CCH_3)_2]^{n+}$ and $[Fe_2(BPMP)(O_2CCH_3)_2]^{n+}$ have been reported to be -0.08 and $+0.60$ V and $+0.01$ and $+0.72$ V vs Ag/AgCl, respectively.[12] In a previous study[20] we reported that the imidazole-containing complex $[Fe_2(BIMP)(O_2CCH_3)_2]^{n+}$ displays two redox steps at -0.18 and $+0.477$ V vs Ag/AgCl. The reduction potential for the PAP_o-PAP_r couple has been reported to be $+0.367$ V vs NHE (about $+0.170$ V vs Ag/AgCl) at pH = 5.00.[32] Compared to the $BIMP^-$, $BPMP^-$, and $BZIM^-$ diiron complexes and PAP, $[Fe_2(BIOMP)(O_2CCH_3)_2]^{n+}$ exhibits a large cathodic shift of the redox potentials due to the presence of two terminal phenolate groups.

Conclusion

A new phenol-containing polyimidazole ligand has been prepared and found to readily stabilize dinuclear iron(III) complexes that resemble the proposed active site structure of purple acid phosphatase proteins. $[Fe_2(BIOMP)(O_2CCH_3)_2]^+$ displays an intense phenolate-to-iron(III) charge transfer transition at 536 nm similar to PAP_o and related model compounds. The two iron(III) centers are weakly coupled antiferromagnetically and display two one-electron redox processes at potentials that are more cathodic compared to that of the $Fe^{III}_2/Fe^{III}Fe^{II}$ couple reported for PAP.[32] These results support the conclusion by others[5] that the redox center in PAP is the iron center that is not coordinated to the tyrosine residue. Finally, future studies will focus on dinuclear iron complexes of unsymmetrical polyimidazole ligands. We recently prepared a new ligand, 2-[bis((1-methylimidazol-2-yl)methyl)aminomethyl]-4-methyl-6-[(2-hydroxybenzyl)((1-methylimidazol-2-yl)methyl)aminomethyl]phenol (H_2BTIMP), which readily stabilizes diiron complexes with metal centers in dissimilar coordination environments. Details of the synthesis and properties of this unique ligand and its metal complexes will be the subject of future reports.

Acknowledgment. This work was supported by National Institutes of Health Grants GM 45783 (R.M.B.) and HL 13652 (D.N.H.).

Supplementary Material Available: For compound **5**, tables giving experimental details of the crystal structure determination, anisotropic thermal parameters, bond distances and angles, hydrogen atom positional parameters, torsion angles, and d.c. magnetic data (19 pages). Ordering information is given on any current masthead page.

IC941250H

(32) Wang, D. L.; Holz, R. C.; David, S. S.; Que, L., Jr.; Stankovich, M. T. *Biochemistry* **1991**, *30*, 8187–8194.